

# **EXPLICIT SIMULATIONS OF WEB TRANSPORT THROUGH PROCESS MACHINES USING PERIODIC MEDIA ANALYSIS TECHNIQUE**

**By**

**Boshen Fu and Neal Michal  
Kimberly-Clark Corporation  
USA**

## **ABSTRACT**

In this paper, the periodic media analysis (PMA) technique in Abaqus/Explicit [1] has been applied to simulate multiple cases of web transport through process machines. The Abaqus models for web transport developed in the Web Handling Research Center (WHRC) at Oklahoma State University (OSU) all have long free upstream spans, which are required to achieve steady state for post-simulation analysis. This increases model size and complexity, induces longer simulation run time and limits applications of simulations. The primary goal of introducing PMA to web handling modeling is to create simulation models which take a shorter time to run. The PMA technique is a Lagrangian technique that offers a Eulerian-like view into a moving structure. Models created using this technique have smaller sizes, and the simulation run time is significantly reduced compared to OSU models [2]. In this work, the moment transfer due to roller misalignment case has been modeled using the PMA technique. The results, e.g. lateral displacements and moment distribution, are compared to OSU model results and experimental results. The comparisons show good agreements. More importantly, the PMA model takes a much shorter time (about 40% less) to conduct. Two more cases, actual wrinkle formation and web with non-uniformity running through rollers, have been modeled using PMA as well. The simulation results from the actual wrinkle formation case agree with the wrinkle failure criterion [3] based upon Timoshenko's shell buckling theory [4]. The web with non-uniformity case indicates the capability of PMA to study complex web structures.

## **INTRODUCTION**

Abaqus/Explicit has been used to model different types of web handling problems: moment transfer due to roller misalignment [2], wrinkle due to moment transfer [3], lateral mechanics of web transiting concaved roller [5] and crowned roller [6], simulations of accumulators [7] and simulations of web behavior due to cross machine direction (CMD) variations[8]. In the last two International Web Handling Conferences,

there were several papers about web handling simulations using Abaqus/Explicit. Though it has been proved to be a very useful analysis tool, Abaqus could be more beneficial improving the web handling industry. One major obstacle that prevents Abaqus from being more popular in web handling research is consuming computational time. With fast development of parallel computing, the simulations could be conducted faster. However, the conventional web transport models still need a long free span to reach steady state, which will take a longer time if more rollers are involved. Additionally, a long free span might cause inconsistent conditions for webs entering rollers when web non-uniformity is included [8]. In this work, a relatively new simulation technique, periodic media analysis in Abaqus/Explicit will be introduced to simulate web instability during transportation. This simulation technique first came out in the Abaqus 6.11 version. PMA is a Lagrangian technique that offers an Eulerian-like view into a moving structure [1]. It can be used to effectively model systems that are repetitive in nature, which makes it very suitable for web transportation simulations. PMA does not require the excessively large meshes that traditional modeling techniques use, which enable it to speed up computational time significantly.

The schematic plots in Figure 1 show the difference between a traditional or OSU model and a PMA model. As shown in Figure 1 (a), an OSU finite element web handling model requires a long free span (usually more than three times of test span) for input to reach steady state. This depends on the length of testing span (distance between two rollers in this figure) and how many rollers are included in the model. Longer free span length has to be added if steady state cannot be achieved. On the other hand, the PMA model uses a different approach. The web length is not critical as long as it can run through the rollers modeled. A trigger plane is required for the PMA model to activate a periodic media procedure as shown in Figure 1 (b). The five blocks shown in Figure 1 (b) runs like a loop during simulation: Block 5 is moved to the upstream side and tie to Block 1 and then Block 4 is moved from the downstream end to the upstream end and so on. By re-using elements that have left the process zone via this shuffling process, the large meshes at the upstream end required for purely Lagrangian simulations can be avoided. There are some special boundary condition set-ups required for the PMA model [1] which will not be described and discussed in this work. If steady state cannot be achieved by a set simulation time, a longer simulation time can be applied without modifying the model's geometry. Because of this special feature, PMA web handling models will save computational time significantly compared to traditional/OSU web handling models.

In following sections, three models will be described and discussed. The first one is a moment transfer simulation using a PMA model and an OSU model. The simulation results will be compared to experimental results reported in [2]. The second one is an actual wrinkle formation simulation using a PMA model to indicate PMA's capability to handle severe deformation. The third case is on web non-uniformity simulation using PMA. In this work, computational time means the amount of time for CPU processing; simulation time means the amount of time set in the simulation models.

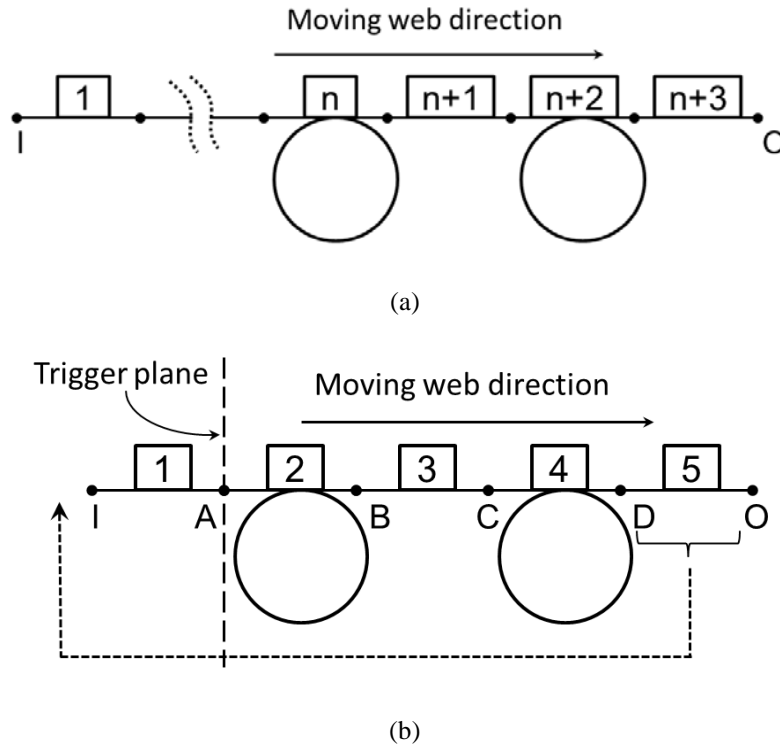


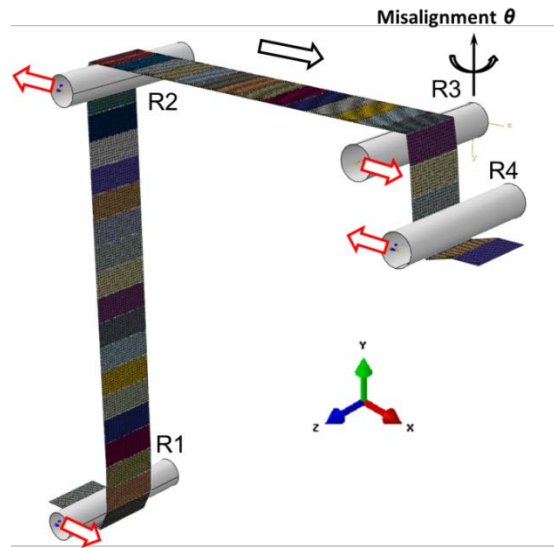
Figure 1 – Schematic plots of web handling models: (a) Traditional/OSU model; (b) PMA model.

## MOMENT TRANSFER DUE TO DOWNSTREAM MISALIGNED ROLLER

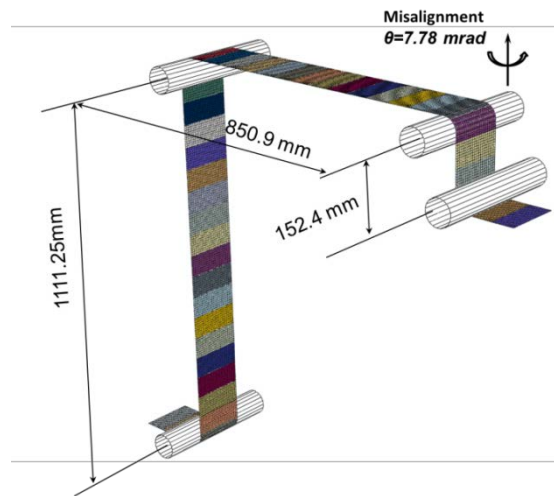
### Finite element models

As described in the last section, a PMA model is composed of blocks. In this moment transfer model, 42 blocks whose dimensions are 152 mm × 63.5 mm are used to generate a web model. As shown in Figure 2, the blocks are shown as different colors. All of the blocks are connected together and form the shape of a web. Since the blocks must be identical, the curvature regions wrapping on the rollers are not initially modeled. As a result, there are two steps in this simulation: simulation times are 0.3s and 150s for 1<sup>st</sup> and 2<sup>nd</sup> steps respectively. 42 blocks form the web shape, but curvature parts are not included in the initial set-up as shown in Figure 2 (a). In Step 1, four rollers will be moved into expected positions (directions shown as arrows in Figure 2 (a)) to match the web span lengths to experimental settings. In addition to that, a 57.8 N tension is applied based upon the test settings [2]. The web tension and contact force will deform the blocks to form the curvature shape wrapping on the rollers. Figure 2 (b) shows the set-up after pre-stretch by moving rollers into expected positions and applying web tension. In Step 1, Roller 3 (R3) will be misaligned simultaneously with roller movements as well. Periodic media analysis stays inactive through Step 1. After pre-stretch, the span lengths shown in Figure 2 (b) are same as the OSU experimental settings [2]. In Step 2, the periodic media analysis will be activated and the web starts moving along the direction shown in Figure 2 (a). General contact is used for interaction between web and rollers: friction coefficient

between web and Roller 1 (R1) and Roller 4 (R4) is 0.9, 0.4 friction coefficient is applied on Roller 2 (R2) and R3. The OSU model will be the same as what is used in [2], except for the general contact for interaction. The reason to use general contact is because it is a more robust contact algorithm and it is also an Abaqus official preferred contact algorithm. All the models will be run in parallel with same amount of CPUs (12) to compare computational time fairly.



(a)



(b)

Figure 2 – Explicit PMA model of a web transiting four rollers: (a) PMA model set-up Step 1; (b) PMA model set-up after Step 1.

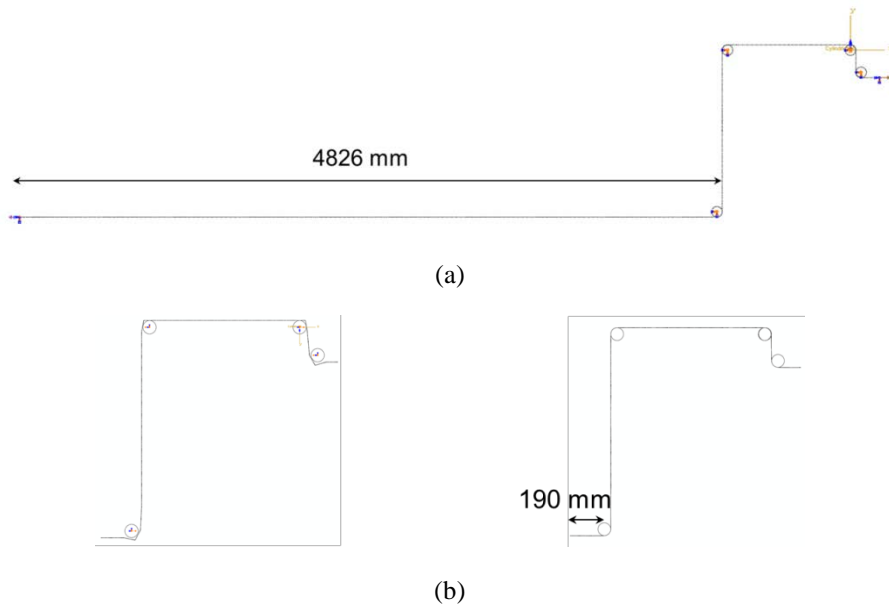


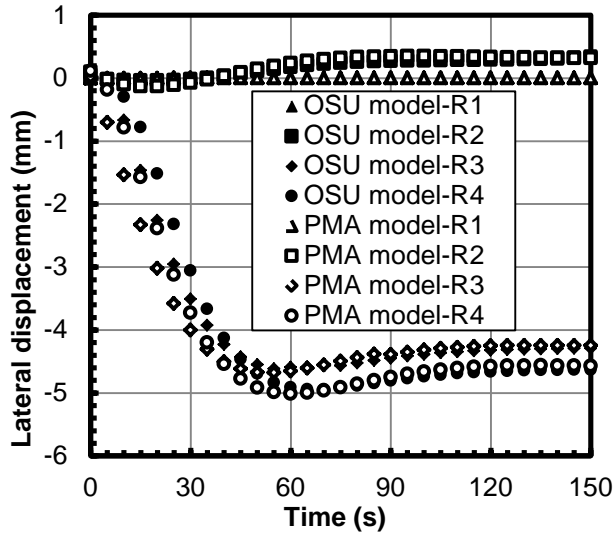
Figure 3 – Model set-up comparison: (a) OSU model with a 4826 mm free span; (b) PMA model with a ~190 mm free span

Side views of the OSU model and the PMA model are shown in Figures 3 (a) and (b) respectively. As described previously, the conventional OSU model requires a long free span. In this case, a 4826 mm long span is required to achieve steady state. The PMA model only requires a 190 mm free span. Element size is the same in both models, which is 6.35 mm  $\times$  6.35 mm. The OSU model is generated by 27,600 elements compared to 10,080 elements in the PMA model. Membrane elements are used in both models which are same as the model set-up in [2]. Young's modulus and Poisson's ratio are 3.93 GPa and 0.3, respectively. The roller diameter is 73.66 mm.

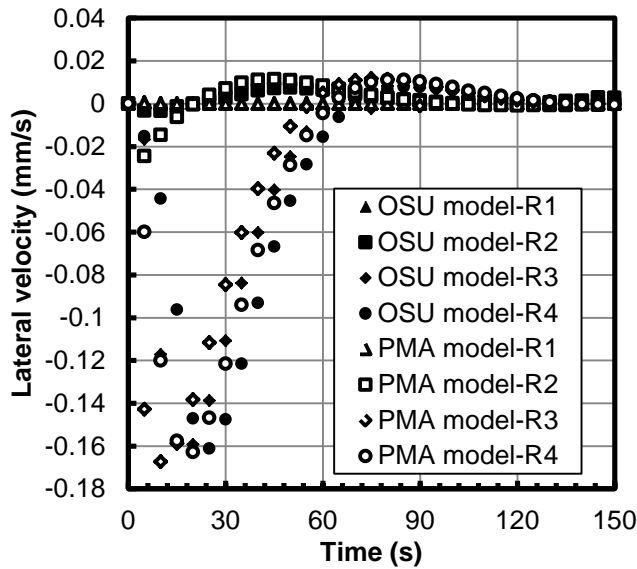
### **Simulation results**

To demonstrate that steady state conditions were reached, the lateral displacements of the web acquired at the entry points of the four rollers and the corresponding velocities are presented in Figure 4. These data were collected on the web centerline (the elastic axis). At the start of the simulations, the lateral deformations of the web are all zero entering each of the four rollers. As the simulation progresses, note that the lateral deformation remains zero as the web enters R1. This is an indication that the moment interaction has been confined to the pre-entering span between R1 and R2 and the entering span between R2 and R3. As the simulation progresses, note the positive lateral deformation of the web at R2 followed by negative deformations at R3 and R4 in both models. The signs of these deformations are with respect to the coordinate axes shown in Figure 2, where a positive misalignment angle is shown. The shape of the deformed web is consistent with the illustration of lateral deformation under moment transfer conditions. The displacements reach steady state after about 120s for both models. As shown in Figure 4 (b), the lateral velocities of the web before entering each roller converge to zero after 120s. Thus, the web does not move laterally any further and steady state behavior has been achieved in both models. The results presented hereafter were harvested from

the last step of the simulations where steady state conditions had been achieved. Due to the pre-stretch step in the PMA model, the lateral displacements and velocities are different in the first 60s between two models, but the results agree with each other after steady state is achieved.



(a)



(b)

Figure 4 – Simulation results comparison (OSU model vs. PMA model): (a) Web lateral displacements at the entry point of each roller; (b) Web lateral velocities at the entry point of each roller.

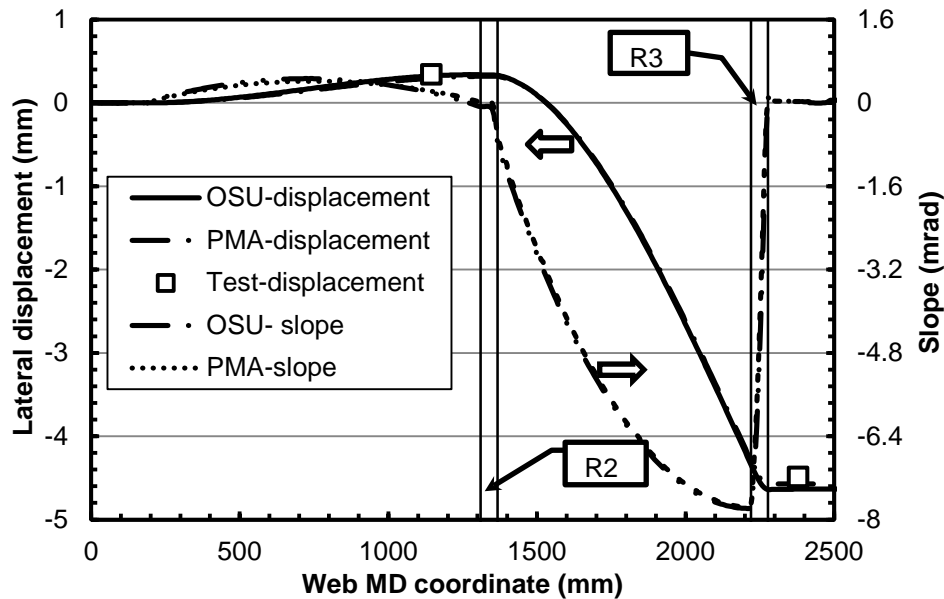


Figure 5 – Comparison of lateral displacement of simulations (OSU model vs. PMA) and experiments and the calculated slope curve for a misalignment at R3 of 7.78 mrad.

The lateral displacements from two simulation models along the centerline of the web are shown in Figure 5. The experimental results agree with the simulation results from both models very well. As shown in Figure 5, the displacements from the two models are identical in the pre-entering span and the entering span. To determine whether normal entry was achieved in the simulations, slopes were calculated using the lateral displacements of the elastic axis of the web shown in Figure 5 and then overlaid in those charts. The slopes were calculated using a finite difference method to approximate the derivative of the lateral displacements with respect to the MD coordinate. The slope is not a direct output for the membrane element because an out-of-plane rotation is not a defined degree of freedom. It is clear in Figure 5 that the slope of the web is equivalent to the misalignment of roller R3 as the web enters R3. Thus the normal entry boundary condition appears to have been achieved as the web enters R3 in PMA model. The lateral deformation of the web on R2 is opposite in direction to the lateral deformations of the web entering R3. It is apparent that span interaction is present and has resulted in lateral deformation in both the pre-entering span and the entering span. The slope of the web at the entry of R2 in Figure 5 is very near zero in both models. Normal entry of the web to R2 is achieved for the range of misalignment of R3 presented here. The slope of the web at the exit of R2 is shown to increase with misalignment in Figure 5.

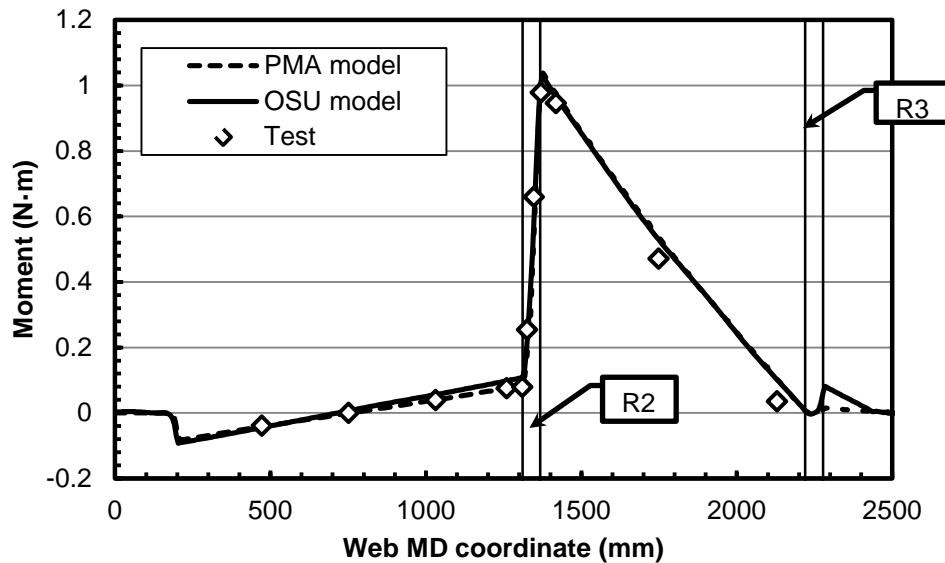


Figure 6 - Moment from simulations and tests for a misalignment for 7.78 mrad at R3.

To compare moment transfer results between the OSU model and the PMA model, internal moments were calculated from the simulations and compared with moments inferred from the LDV test data [2] in Figure 6. The steady state MD stresses from the two models were used to estimate the internal moment in the web at MD locations using the equation,

$$M = \int \sigma_{MD} z dA \approx \sum_{i=1}^n \sigma_{MDi} z_i A_i \quad \{1\}$$

where  $\sigma_{MDi}$ ,  $z_i$ , and  $A_i$  are the MD stress levels at the nodes, the distances between the nodes and the elastic axis, and the cross-sectional area of the web associated with the nodes, respectively. Also shown in Figure 6 are the moments inferred in tests using the LDVs reported in [2]. Each data point shown is the average of ten measurements and the standard error of the data was 0.01 N·m or less. The simulation results from both models agree with experimental results very well at each point. The moment reaches its peak value at the exit for R2 and then decreases almost linearly as the web approaches R3 in the entering span. Eventually, the moment decreases to zero when the web arrives at the misaligned roller R3 and is consistently zero on the roller until the web exits R3. The PMA model indicates slight differences with the OSU model in the pre-entering span. In fact, it produces closer results to experimental data. In the entering span, the two simulation models produce identical moment results. After the web exits R3, moments calculated using MD stresses from periodic model are close to zero, which are more consistent compared to the OSU model.

	OSU model	PMA model
Computational time	9 hour 13 minutes	5 hours 38 minutes

Table 1 – Computational time



The simulation results of lateral displacement, slope and moments at different locations from the PMA model agree with experimental results and simulation results using the conventional OSU model. The PMA model takes much less computational time to conduct. For the cases shown herein, the computational time is shown in Table 1. The PMA model only takes about 60% of the computational time of the OSU model. The simulation time in this case is 150 seconds, which is determined by the free span length in the OSU model. If a longer simulation time is needed to achieve steady state status, the only way is to increase the free span length for the OSU model, which will increase computational time significantly because of having more elements involved. On the other hand, the PMA model does not require any modification of geometric structure and the number of elements will remain same, which means computational time will not be affected much by increasing simulation time.

### **SIMULATION OF ACTUAL WRINKLE FORMATION DUE TO ROLLER MISALIGNMENT**

Timoshenko's shell buckling theory has been used to develop a wrinkle failure criterion: when CMD compressive stresses at the entry to a roller are higher than the compressive stress calculated using Timoshenko's shell buckling stress as shown in equation {2}, a wrinkle will start forming. This criterion has been combined with relatively coarsely meshed models to predict wrinkle formation to save computational time successfully [3]. The focus of this simulation is to use the PMA model to simulate actual wrinkle formation and compare CMD stress distribution to the wrinkle failure criterion. Simulation results will indicate the capability of PMA to model complex deformation, such as severe distortion of elements during wrinkling.

To model actual wrinkle formation due to roller misalignment, a four-roller narrow web model was employed to examine the CMD stresses in the web near the entry to the misaligned roller. In this simulation, the mesh size must be extremely small to capture the actual wrinkle formation. If the CMD stress is close to Timoshenko's theory at where the wrinkle appears, capability of the PMA model to deal with severe element deformation could be demonstrated and PMA will be employed in future similar analyses. The PMA model of this simulation is shown in Figure 7. Young's modulus and Poisson's ratio are 4.9 GPa and 0.3 respectively. A high friction coefficient, which is equal to 4, is used between R2 and the web to avoid unexpected web slippage on the roller. A friction coefficient of 1 is used for the contact between the web and other rollers. The same as the moment transfer PMA model, this simulation includes two steps as well. In the first step, the blocks will be pre-stretched by moving rollers into expected positions. R3 will be misaligned by 75 mrad in the 1<sup>st</sup> step to generate enough shear force to form wrinkle. The analytical rigid rollers and shell element (S4R) web were used in the simulations.

$$\sigma_{cr} = \frac{-Et}{R\sqrt{3(1-\nu^2)}} \quad \{2\}$$

$$\lambda = 3.44 \cdot \sqrt{Rt} \quad \{3\}$$

Since the wrinkle wavelength is very small, a really fine mesh must be used to simulate actual wrinkle formation. The wrinkle wavelength  $\lambda$  can be calculated using equation {2}, where  $R = 36.83$  mm is the radius of roller and  $t = 0.023$ mm is the thickness of web. Using equation {3}, the calculated wavelength is 3.19 mm for this

material and model set-up. To capture wrinkles on the misaligned roller, more than two elements are expected in one wave. Accurate results should be achieved using a small element size, which leads to an extremely fine mesh with a size of  $0.635 \text{ mm} \times 0.635 \text{ mm}$  used in this simulation. A  $22.24 \text{ N}$  tension was applied on the upstream end, and a  $76.2 \text{ mm/s}$  velocity was applied on the downstream end. Both tension and velocity were ramped up from zero to the set value in the 1<sup>st</sup> step of the simulation, which will take  $0.3 \text{ s}$ , and stay constant in the 2<sup>nd</sup> step. The total simulation time for the second step is  $5 \text{ s}$ .

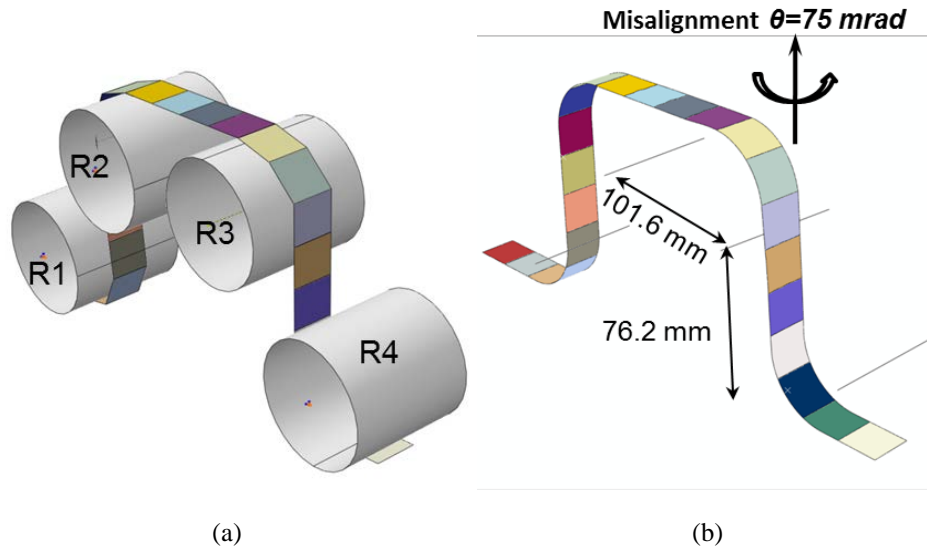


Figure 7 – PMA model used for wrinkle formation simulation: (a) Initial model set-up; (b) span lengths and misalignment after pre-stretch step.

The simulation results of CMD stress distribution at two different time steps are shown in Figures 8 (a) and (b). According to the wrinkle failure criterion statement, when the CMD stress near the entry point to R3 reaches the critical stress calculated using equation {2} which is  $-1.89 \text{ MPa}$  in this case, the wrinkle would start forming on R3. Figure 8 shows the step where wrinkle starts forming (b) and a step  $0.025 \text{ s}$  earlier (a). In Figure 8 (a), the CMD stresses in the web start to form a high value zone near the entry point to R3. In Figure 8 (b), the wrinkle already started propagating along the MD direction and CMD stresses became much higher, caused by bending due to wrinkle formation. Figure 8 may not be clear enough to show the exact stress values at the entry to R3.

To accurately identify CMD stresses at the entry to R3, contact pressure will be used. The contour plots in Figures 9 (a) and (d) are CPRESS distributions before and after wrinkle formation. In Abaqus, CPRESS is defined as the contact pressure between two different parts. There will only be zero value for the area without contact as shown in Figure 9. Per CPRESS contour plots, the wrinkle starts at a step time equal to  $0.641 \text{ seconds}$ , and propagates further in the following steps. It is clearly seen that the zero contact pressure distribution moves further in Figures 9 (c) than (a), which means the web lifts more to induce out-of-plane deformation due to wrinkle formation. Four rows of nodes near the entry were selected for each case as shown in Figures 9 (a) and (d). The

CMD stresses acquired along these four lines are plotted in the charts in Figures 9 (b) and (c). In the Figure 9 (b) chart, the four CMD stress curves are close to each other and the peak values are all around the critical stress, -1.89 MPa, which is presented as a red solid horizontal line. It indicates that the stress condition to generate a wrinkle is already satisfied at this step and wrinkle formation has started. Figure 9 (c) shows the CMD stresses are much higher than -1.89 MPa because the wrinkle occurs and causes higher CMD stresses due to the bending of the web.

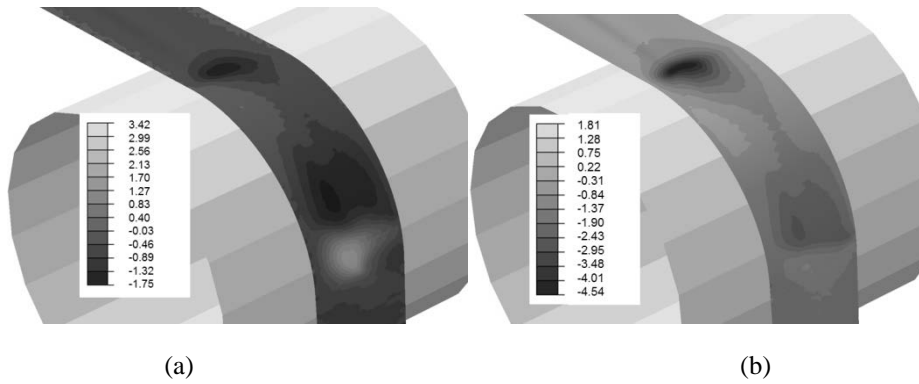
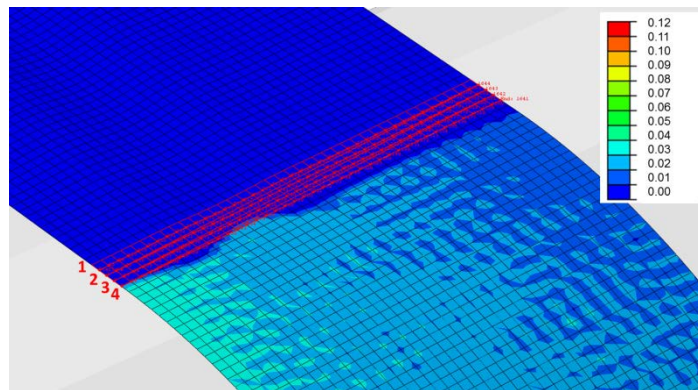
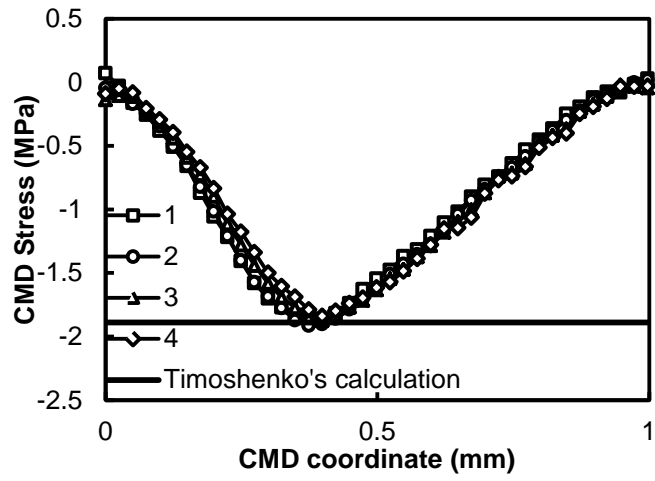
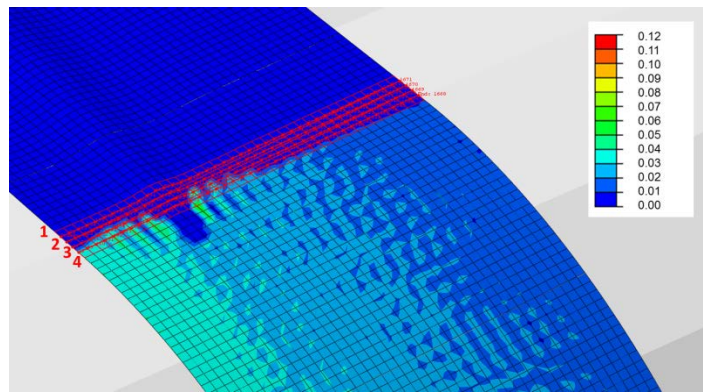


Figure 8 – Minimum principal stress distributions: (a) Step time = 0.625 s; (b) Step time = 0.65 s.

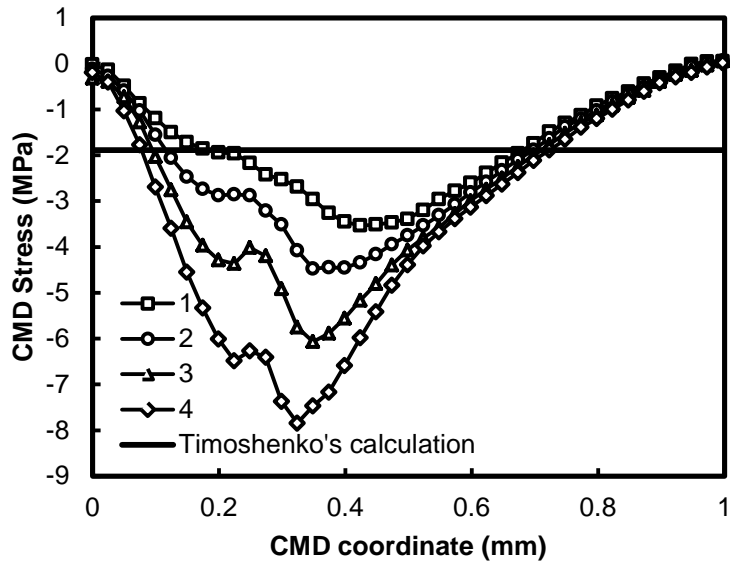




(b)

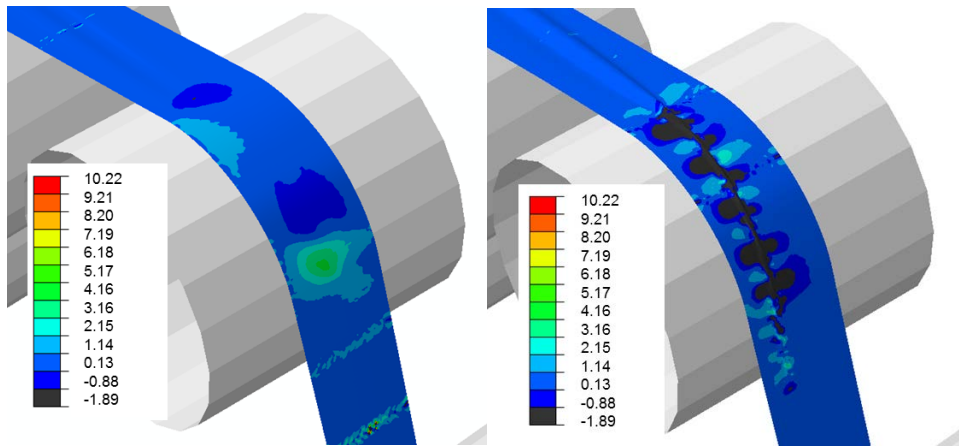


(c)



(d)

Figure 9 – Contact pressure and CMD stress distribution near the entry point of web to the roller: (a) Contact pressure at step time = 0.641 s; (b) CMD stresses distribution at step time=0.641s; (c) Contact pressure at step time = 0.875 s; (d) CMD stresses distribution at step time=0.875s.



(a)

(b)

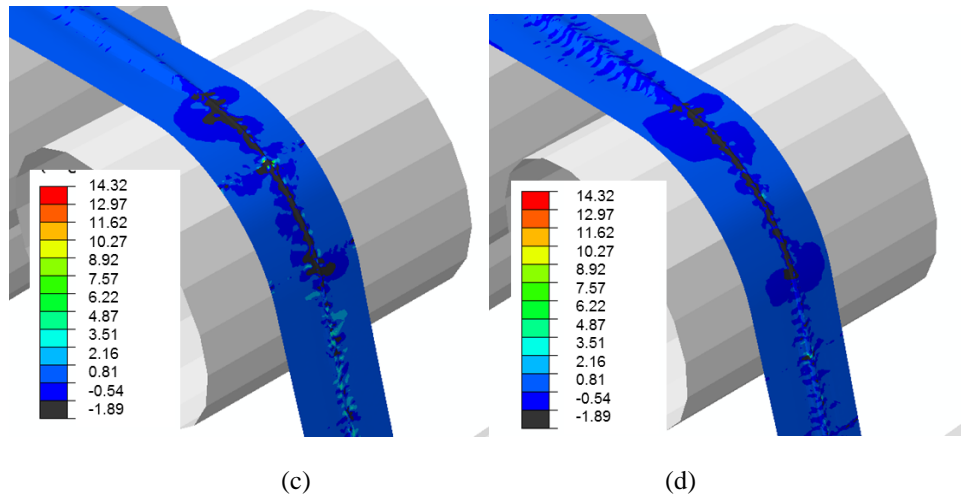
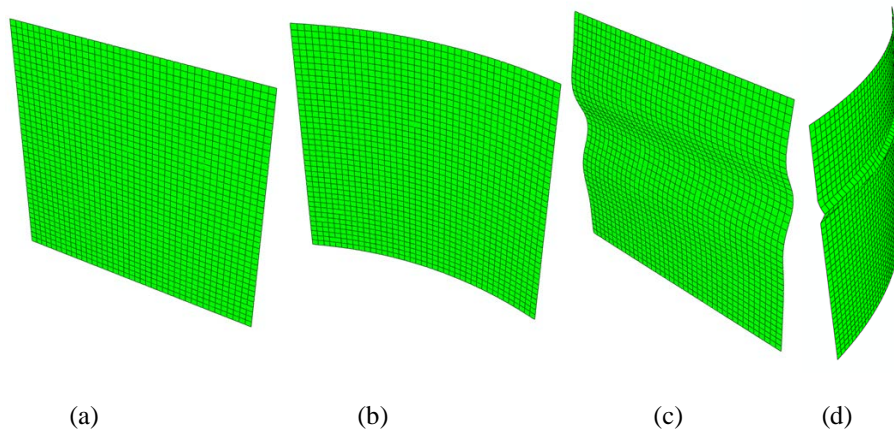


Figure 10 – CMD stress distribution at different step time (a)  $t = 0.641$  s; (b)  $t = 2$  s; (c)  $t = 4$  s; (d)  $t = 5$  s.

Figure 10 shows the CMD stress distributions at following steps. To present Timoshenko's theory more clearly, a threshold value (-1.89 MPa) was set to plot these contours. In this case, the black color represents the stresses are negatively higher than -1.89 MPa. At Figure 10 (a), the high stress concentration zone is forming and troughs are converting to wrinkles only near the entry point. In Figures 10 (b), (c) and (d), the wrinkles are generated and propagate along the machine direction on the roller and then to the existing span. As shown in Figure 10, the black color starts at the entry point and moves with wrinkle propagation on the roller. It means that critical CMD stresses, which could be predicted using Timoshenko's theory, generate at the entry point to roller, and become much higher in the web on the roller, which supports the wrinkle failure criterion.



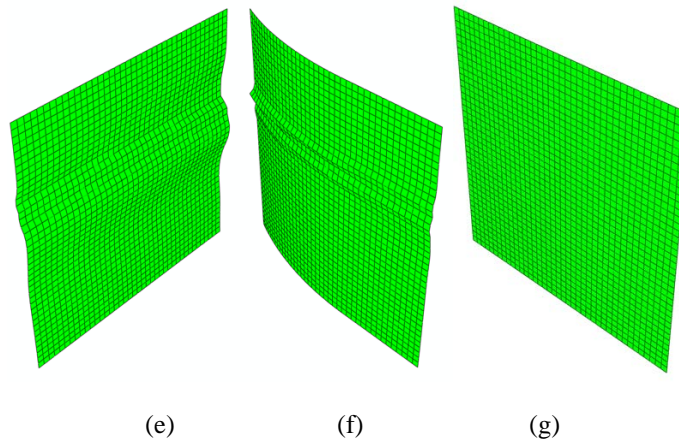


Figure 11 – Deformation of one block through the simulation: (a) time=0s; (b) time=0.3s; (c) time=1s; (d) time=2s; (e) time=3s; (f) time=4s; (g) time=5s.

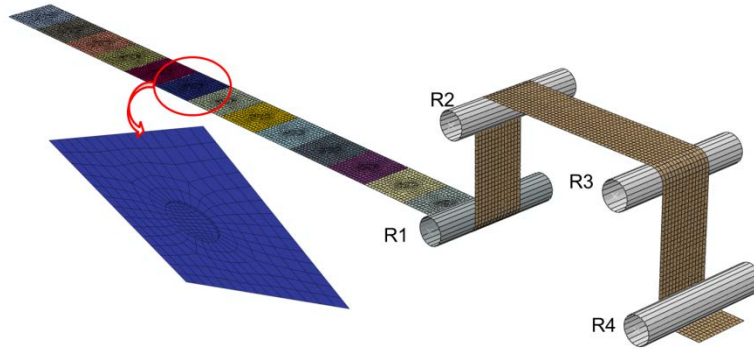
Deformations of one block at different times through the simulation are shown in Figure 11. At the initial state in Figure 11 (a), the block is a flat sheet. After pre-stretch step (b), the block is wrapped on one of the rollers and has a curvature shape. After 1s of simulation time as shown in (c), a trough is generated in this block due to misalignment of R3. At 2s shown in (d), a wrinkle has been generated in the block. At following steps shown in (e) and (f) and the wrinkle will maintain until the block moves back to the upstream end as shown in (g). This indicates that PMA is capable of dealing with severe deformation of elements during simulation and this deformation will not affect the input conditions of the block when it moves back upstream.

#### **SIMULATION OF WEB TRANSPORT AFFECTED BY WEB NON-UNIFORMITY**

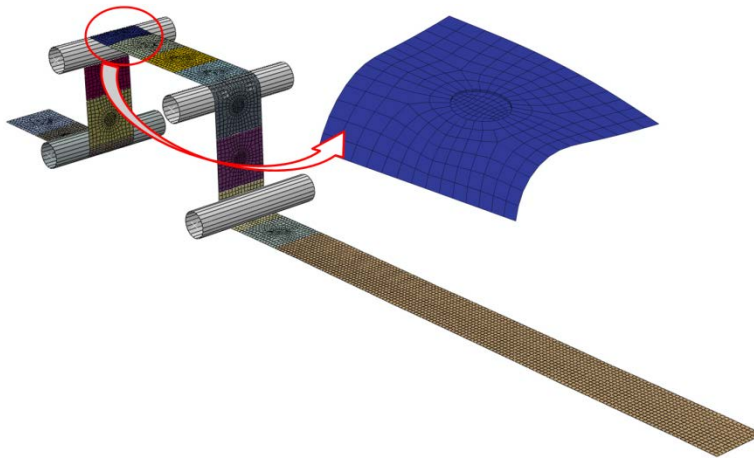
PMA could be used to model more complex web structures as well. In this section, a PMA model to simulate the effect of web non-uniformity will be introduced. Instead of using the model set-up approach shown in last two sections, a different model set-up method has been used. As shown in Figure 12 (a), PMA blocks follow the web wraps on four rollers. This is similar to the process of threading a belt wrapping through rollers, which is same as the start of a realistic manufacturing process. Each PMA block has a thick circle area in the center. In this model, shell elements (S4R) are used to model the web and the thickness is 0.0762 mm; solid elements are used to generate the thick area which is 0.508 mm. The initial geometry of the PMA block is shown in Figure 12 (a) and each block is shown as a different color. The web will run through four rollers and move the PMA blocks into the right positions as shown in Figure 12 (b). Deformed geometry of the same PMA block shown in (a) is shown in (b) as well. Then the periodic media part of the mesh will be imported into a separate model without leading mesh as shown in (c). This model will be used to conduct periodic media analysis. The simulation time for this PMA is 20s. Young's modulus is 689 MPa and Poisson's ratio is 0.4. The PMA block dimension is 50.8 mm × 50.8 mm and the thicker circle radius is 6.35 mm. The web tension is 4.45 N.

Stress distributions are shown in Figure 13. Two simulation times are shown in this figure: 19s and 20s respectively. Both maximum and minimum in-plane stresses are

shown to indicate the effect of non-uniformity. Before the thicker dot moves into roller R3, the compressive stress generated on the roller is not high as shown in Figure 13 (b). But when the thicker dot is moving on the roller R3, it generates higher compressive stress near the entry to R3 as shown in Figure 13 (d), which can potentially cause wrinkle formation. Another benefit of the PMA model is a consistent condition to enter R1 because there is a relatively consistent short free span. This avoids issues caused by inconsistencies associated with long free span and web non-uniformity [8].

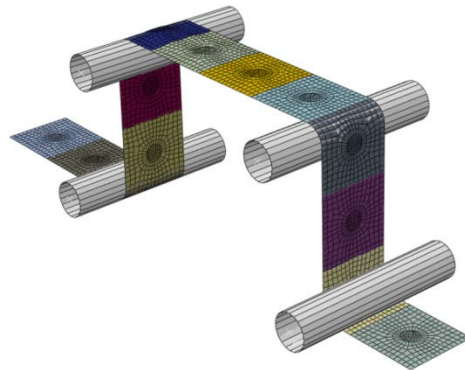


(a)



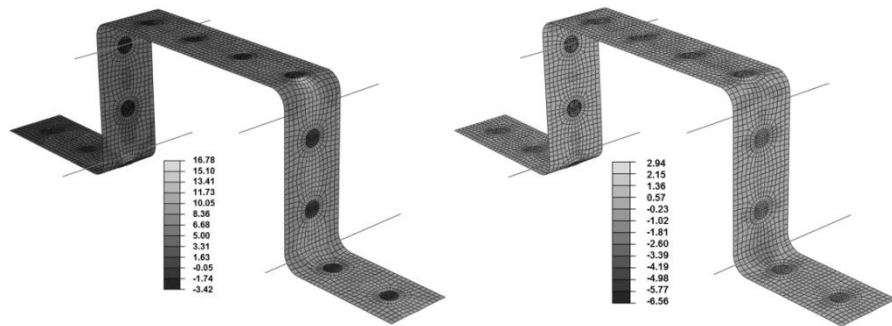
(b)





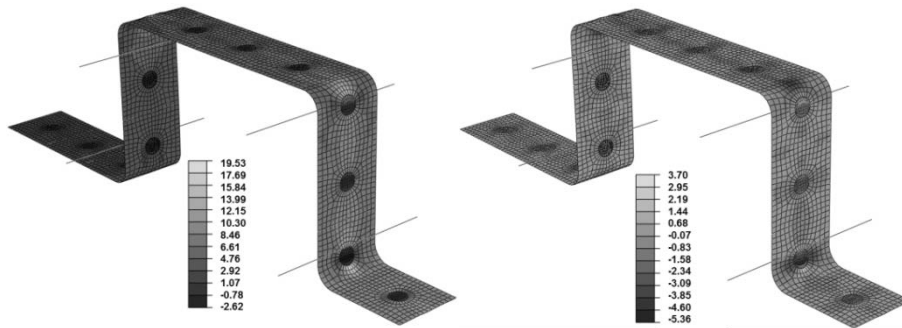
(c)

Figure 12 – Model set-up: (a) Initial model set-up; (b) Periodic media blocks moved into positions; (c) PMA model generated using deformed blocks shown in (b).



(a)

(b)



(c)

(d)

Figure 13 – Stress distribution at different simulation times: (a) Maximum in-plane stress at simulation time=19s; (b) Minimum in-plane stress at simulation time=19s; (c) Maximum in-plane stress at simulation time=20s; (d) Minimum in-plane stress at simulation time=20s.

## CONCLUSIONS

Simulation results from moment transfer simulations using the PMA model agree with results from the OSU model and experimental data. PMA is much more efficient in term of computational time to deal with web transportation and produces accurate results. PMA can be used to model actual wrinkle formation. CMD compressive stresses from the simulation PMA model agree with the wrinkle failure criterion, which demonstrates the capability of PMA to simulate complex contact and severe deformation behaviors. Complex web structures, such as non-uniform thickness, are able to be modeled using PMA as well. Periodic media analysis has great potential to benefit the web transportation related simulations. It will take much less computational time to conduct simulations. Using PMA, models can be generated to focus on the modules where issues occur without a long free span included. This also makes the control of web conditions of entering the first roller easier. PMA models can avoid inconsistent conditions when webs enter the first roller due to change length of free span associated with web non-uniformity, such as camber and thickness variation. Overall, PMA technique is a powerful feature of Abaqus but it requires good engineering judgment to determine when it should be employed to simulate web handling related problems.

## REFERENCE

1. Abaqus Analysis User's Manual, Section 10.5, 2014.
2. Fu, B., Reddy, A., Vaijapurkar, S., Markum, R. and Good, J. K., "Boundary Conditions that Govern the Later Mechanics of Flexible Webs in Roll to Roll Process Machines," ASME Journal of Computational and Nonlinear Dynamics, Vol.9, 2014.
3. Fu, B. and Good, J. K., "Web Wrinkling Resulting from Moment Transfer", Proceedings of the Twelfth International Conference on Web Handling, Web Handling Research Center, Stillwater, Oklahoma, June, 2013.
4. Timoshenko, S. P., and Gere, J. M., Theory of Elastic Stability, 1<sup>st</sup> Ed. McGraw-Hill, New York, 1987.
5. Vaijapurkar, S. and Good, J. K., "Explicit Analysis of Lateral Mechanics of Webs Transiting a Concave Roller," Proceedings of the Eleventh International Conference on Web Handling, Web Handling Research Center, Stillwater, Oklahoma, June, 2011.
6. Vaijapurkar, S., Beisel, J. A., and Good, J. K., "The Behavior of Webs Transiting Crowned Rollers," Proceedings of the Twelfth International Conference on Web Handling, Web Handling Research Center, Stillwater, Oklahoma, June, 2013.
7. Kandadai, B. K., Michal, N., and Patil, A., "Analysis of Web Wrinkling in Accumulators," Proceedings of the Eleventh International Conference on Web Handling, Web Handling Research Center, Stillwater, Oklahoma, June, 2011.
8. Lange, S., Looney, M., and Carrle, J., "Lateral Dynamics Simulations of Webs Having Cross-Machine Direction Variation," Proceedings of the Twelfth International Conference on Web Handling, Web Handling Research Center, Stillwater, Oklahoma, June, 2013.